DOI: 10.1002/chem.200801203

Oxidation by Oxygen and Sulfur of Tin(IV) Derivatives Containing a Redox-Active *o*-Amidophenolate Ligand

Alexandr V. Piskunov,*[a] Irina N. Mescheryakova,[a] Georgii K. Fukin,[a] Evgenii V. Baranov,[a] Markus Hummert,[b] Andrei S. Shavyrin,[a] Vladimir K. Cherkasov,[a] and Gleb A. Abakumov[a]

Abstract: Oxidation of tin(IV) *o*-amidophenolate complexes $[Sn(ap)Ph_2]$ (**1**) and $[Sn(ap)Et_2(thf)]$ (**2**) (ap = dianion of 4,6-di-*tert*-butyl-*N*-(2,6-diisopropylphenyl)-*o*-iminobenzoquinone (ImQ)) with molecular oxygen and sulfur in toluene solutions was investigated. The reaction of oxygen with **1** at room temperature forms a paramagnetic derivative $[Sn(isq)_2Ph_2]$ (**3**) (isq = radical anion of ImQ) and diphenyltin(IV) oxide $[\{Ph_2SnO\}_n]$. Interaction of **1** with sulfur gives another monophenyl-substituted paramagnetic tin(IV) complex, [Sn(ap)(isq)Ph] (**4**), and the sulfide, $[Ph_3Sn]_2S$. The oxidation of **2** with oxygen and with sulfur proceeds through the derivative $[Sn(isq)_2Et_2]$ (**7**), which undergoes alkyl elimination to give two new tin(IV) compounds, [Sn(ap)(isq)Et] (**5**) and [Sn(ap)-(EtImQ)Et] (**6**) (EtImQ = 2,4-di-*tert*-butyl-6-(2,6-diisopropylphenylimino)-3-ethylcyclohexa-1,4-dienolate ligand), respectively, along with the corresponding alkyltin(IV) oxide and sulfide. Complexes **3**–**5** and **7** were studied by EPR spectroscopy. The structures of **3**, **4** and **6** were investigated by X-ray analysis.

Keywords: N,O ligands · oxidation · reaction mechanisms · structure elucidation · tin

Introduction

The main-group metals, with few exceptions, are incapable of changing their oxidation state in complexes, making such common and important processes in transition-metal chemistry as oxidative addition and reductive elimination impossible. These reactions of transition-metal derivatives permit their application in a large variety of organic molecule transformations, including catalytic reactions. However it is possible to simulate the specific reactivity of transition-metal coordination and organometallic compounds by non-transition-metal derivatives by including a redox-active ligand in a main-group-metal complex. The best known such ligands are *o*-quinones, *o*-iminoquinones, diimines, and their derivatives. Redox-active ligands can accept one, two, or more electrons reversibly without loss of coordination to the metal. Thus a redox-active ligand bonded to a main-group-metal ion is able to reduce or oxidize a substrate coordinated to the metal.

The chemistry of non-transition-metal complexes with redox-active ligands has progressed in recent years. There are some striking examples of emulation of transition-metal complex reactivity by main-group-metal complexes. For instance, diiminoacenaphthene (bian) derivatives of magnesium are known to undergo addition reactions with alkyl halides, ketones, nitriles, or C–H acids.[1] Solvent-induced alkyl radical elimination has been observed upon treatment of the complex $[Mg(bian)(iPr)(Et_2O)]$ with THF.[1e] The opposite reaction, radical fixation, is known for the complexes of Group 14 elements with *o*-quinone or diazabutadiene ligands.[2] This property makes it possible to use tin(IV) catecholate derivatives as the controlling agents in olefin polymerization.[3] Unique reversible binding of molecular oxygen by catecholate and *o*-amidophenolate antimony compounds has been observed.[4a–c] This interaction leads to endoperoxo antimony derivatives (Scheme 1). The unprecedented example of a Ga^{III}-radical-mediated reaction that involves the activation of two C–H bonds in redox-active N-

[a] Dr. A. V. Piskunov, I. N. Mescheryakova, Dr. G. K. Fukin, E. V. Baranov, Dr. A. S. Shavyrin, Prof. Dr. V. K. Cherkasov, Prof. Dr. G. A. Abakumov
G.A. Razuvaev Institute of Organometallic Chemistry
Russian Academy of Sciences, 49 Tropinina Street
603950 Nizhny Novgorod (Russia)
Fax: (+7) 831-462-74-97
E-mail: pial@iomc.ras.ru

[b] Dr. M. Hummert
Institut für Chemie der Technischen Universität Berlin
Straße des 17. Juni 135, 10623 Berlin (Germany)

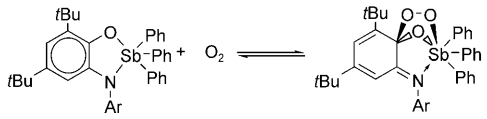

Scheme 1. Reversible binding of molecular oxygen by an *o*-amidophenolate antimony complex.

substituted 2-aminophenolate ligands was reported recently.[4d]

In the present study we investigated the reactions of *o*-amidophenolate tin(IV) derivatives [Sn(ap)Ph_2] and [Sn(ap)Et_2(thf)] (ap = dianion of 4,6-di-*tert*-butyl-*N*-(2,6-diisopropylphenyl)-*o*-iminoquinone) with molecular oxygen and elemental sulfur.

Results and Discussion

The oxidation of [4,6-di-*tert*-butyl-*N*-(2,6-diisopropylphenyl)-*o*-amidophenolato]diphenyltin(IV) (**1**) with molecular oxygen in toluene solution at room temperature is accompanied by a color change from light yellow to deep green. The fine white precipitate forms in a few minutes. EPR analysis of the reaction mixture shows the presence of paramagnetic species. The anisotropic spectrum in a frozen toluene matrix is typical of diradical derivatives (Figure 1a). At 150 K, it exhibits a half-field signal ($\Delta m_s = 2$) characteristic of a diradical. From the zero-field splitting parameters of the $g = 2$ EPR signal (toluene, $D = 209$ G, $E = 6$ G, Figure 1), the unpaired electron separation of 5.10 Å can be estimated. These parameters are comparable with those obtained for dichlorobis[-4,6-di-*tert*-butyl-*N*-(2,6-diisopropylphenyl)-*o*-iminosemiquinonato]tin(IV).[2f]

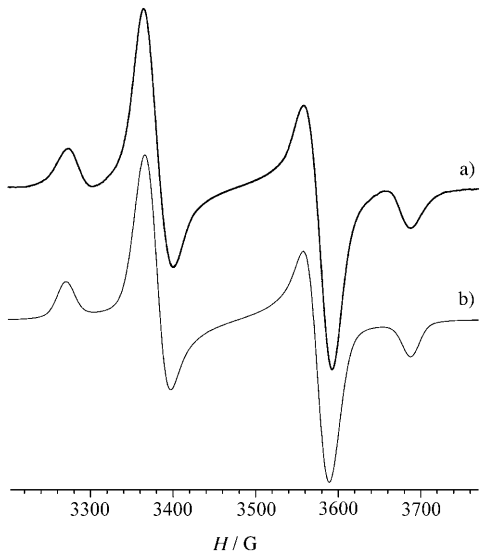

Figure 1. Experimental X-band EPR spectrum of **3** in a toluene matrix a) at 150 K and b) its simulation.

The insoluble white compound was identified as diphenyltin(IV) oxide. Crystallization from hot hexane of the foamy residue remaining after solvent removal afforded bis[4,6-di-*tert*-butyl-*N*-(2,6-diisopropylphenyl)-*o*-iminosemiquinonato]-diphenyltin(IV) (**3**) as dark green crystals in 74% yield (Scheme 2). The structure of **3** was determined by X-ray diffraction studies.

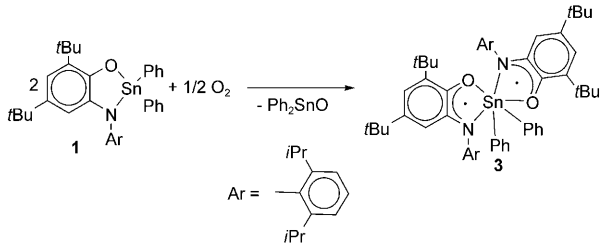

Scheme 2. The reaction of complex **1** with oxygen.

The reaction of **1** with elemental sulfur in toluene under moderate heating was complete after 8 h at 60 °C. The resulting green solution produces a well-resolved isotropic X-band EPR spectrum (Figure 2). The hyperfine structure arises from hyperfine coupling (HFC) of unpaired electron with magnetic nuclei ^{1}H (99.98%, $I = 1/2$, $\mu_N = 2.7928$), ^{14}N (99.63%, $I = 1$, $\mu_N = 0.4037$), ^{117}Sn (7.68%, $I = 1/2$, $\mu_N = 1.000$), and ^{119}Sn (8.58%, $I = 1/2$, $\mu_N = 1.046$).[5] The splitting parameters are: $A_i(^1H) = 2.2$ G, $A_i(^{14}N) = 3.6$ G, $A_i(^{119}Sn) = 28.3$ G, $A_i(^{117}Sn) = 27.1$ G ($g_i = 2.0024$). The observation of HFC with two nitrogen and two hydrogen atoms indicates fast migration of an unpaired electron between two *o*-iminoquinone ligands bonded with the tin atom. One of these ligands is a radical anion and the other is a dianion. This interligand electron exchange is also confirmed by ^{14}N and ^{1}H HFC constants which are nearly two times lower than for the [SnCl(isq)Ph_2] (isq = radical anion of the 4,6-di-*tert*-butyl-*N*-(2,6-diisopropylphenyl)-*o*-iminobenzoquinone) complex.[6]

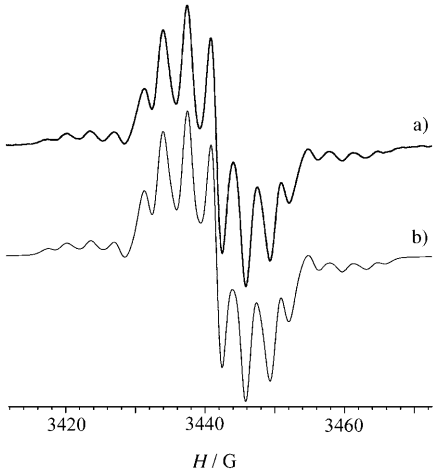

Figure 2. Experimental X-band EPR spectrum of **4** in hexane a) at 290 K and b) its simulation.

The EPR spectrum stays unchanged in character over the temperature interval 220–300 K. In the NIR spectrum, the low-energy band at $\lambda = 1800$ nm can be assigned to a spin- and dipole-allowed LLCT (ligand-to-ligand charge transition) between the MOs of *o*-iminoquinone ligands. Such transitions are usual for mixed-valence transition-metal complexes containing *o*-quinoid ligands in different redox states,[7] but attempts to observe this transition for similar non-transition-metal derivatives were unsuccessful.[7c] These spectral features have led us to propose the formation of an [Sn(ap)(isq)Ph] derivative **4** (Scheme 3).

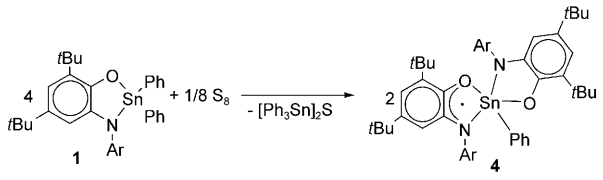

Scheme 3. The reaction of complex **1** with sulfur.

The reactions of the ethyl-substituted *o*-amidophenolate tin(IV) derivative **2** with oxygen and sulfur proceed under conditions analogous to those for **1**. The resulting solutions exhibit EPR activity. The interaction with oxygen is accompanied by precipitation of diethyltin(IV) oxide as a fine white deposit. In both cases (reactions with oxygen and with sulfur) the reaction mixtures have identical well-resolved EPR spectra (Figure 3) which are similar to that observed

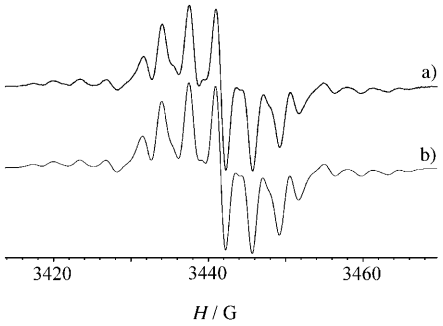

Figure 3. Experimental X-band EPR spectrum of **5** in hexane a) at 290 K and b) its simulation.

for **4**. The hyperfine structure arises from HFC of unpaired electrons with magnetic nuclei ^{1}H, ^{14}N, ^{117}Sn, and ^{119}Sn. The splitting parameters are: $A_i(^{2}H) = 2.2$ G, $A_i(^{2}{}^{14}N) = 3.5$ G, $A_i(^{117}Sn) = 27.5$ G, $A_i(^{119}Sn) = 28.8$ ($g_i = 2.0034$). These spectra should be attributable to [4,6-di-*tert*-butyl-*N*-(2,6-diisopropylphenyl)-*o*-amidophenolato)-[4,6-di-*tert*-butyl-*N*-(2,6-diisopropylphenyl)-*o*-iminobenzosemiquinonato]ethyltin(IV) (**5**). However, we were unable to isolate this minor product from the reaction mixture. The main product of the oxidation of **2** with oxygen and sulfur was the diamagnetic tin(IV) derivative (**6**) (Scheme 4). After removal of volatiles it was isolated by recrystallization of crude product from hexane in about 50% yield. The structure of **6** was determined by X-ray analysis.

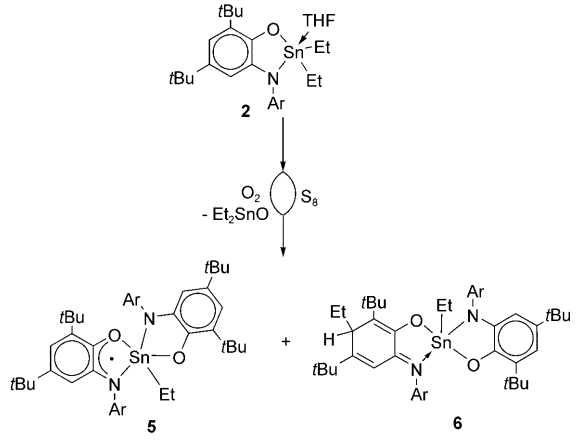

Scheme 4. The reactions of complex **2** with oxygen and sulfur.

The IR spectrum of **6** contains a sharp band at 1615 cm^{-1}, belonging to a stretching vibration $\tilde{\nu}$(C=N) of the coordinated imino group (the IR spectrum of the starting *o*-iminoquinone has this ν(C=N) band at 1635 cm^{-1}[9]).

A mechanism of the oxidation of *o*-amidophenolate tin(IV) derivatives with molecular oxygen has been worked out. According to the known scheme for transition metals,[10] the first step consists of the formation of the superoxo adduct (**8**). In the case of the tin complexes, however, in contrast to transition-metal derivatives, this step includes the oxidation not of the metal center but of the redox-active *o*-amidophenolate ligand, and leads to the diradical product. The superoxo complex can react further with a second *o*-amidophenolate metal derivative to give the μ-peroxo species **9**. The latter can cleave itself to produce free *o*-iminoquinone (ImQ) and oligomeric diorganotin(IV) oxide. In the next step the *o*-iminoquinone oxidizes another molecule of the *o*-amidophenolate derivative forming a bis-*o*-iminosemiquinonatodiorganotin(IV) (Scheme 5).

In the case of phenyl-substituted tin derivatives the final product is a stable complex **3**. Meanwhile the presence of ethyl substituents bonded to the tin atom makes this diradical species unstable and the further transformation of the latter gives **5** and **6**. Additional experiments have confirmed the latter assertion. The solution of **2** in toluene was frozen after exposure to air. The anisotropic EPR spectrum at this stage shows signals typical of diradical derivatives. The zero-splitting parameters ($D = 219$ G, $E = 6$ G) are very close to those observed for **3**, and indicate formation of bis[4,6-di-*tert*-butyl-*N*-(2,6-diisopropylphenyl)-*o*-iminosemiquinonato]-diethyltin(IV) (**7**). Moreover, the reaction of **2** with an equimolar quantity of 4,6-di-*tert*-butyl-*N*-(2,6-diisopropylphenyl)-*o*-iminobenzoquinone as well as the interaction of 2 equiv of *o*-iminosemiquinonatolithium with dichlorodi-

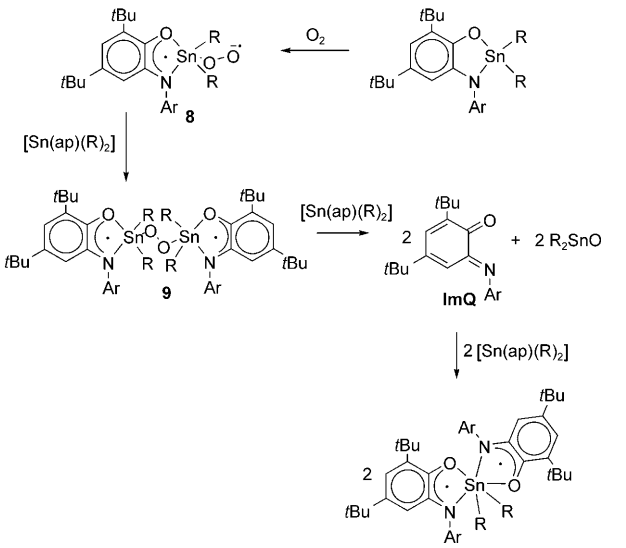

Scheme 5. The probable mechanism of the reaction of *o*-amidophenolate tin derivatives with oxygen.

ethyltin(IV) leads to **7**, which is evident by EPR spectroscopy. The diradical species synthesized undergoes intermolecular rearrangement to give diamagnetic **6** in 2 h (Scheme 6).

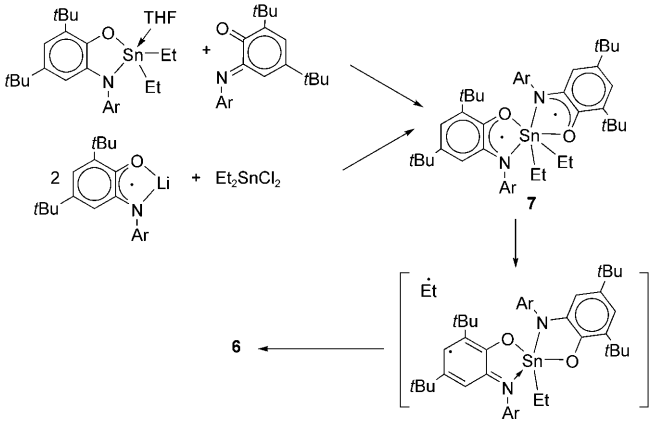

Scheme 6. The generation and transformation of bis(4,6-di-*tert*-butyl-*N*-(2,6-diisopropylphenyl)-*o*-iminosemiquinonato)diethyltin(IV) (**7**).

This rearrangement includes elimination of an ethyl radical and subsequent recombination of a radical pair. The similarity of products observed in reaction of **2** with sulfur to those obtained in reaction with oxygen argues for these processes having related mechanisms.

Our lack of success in the observation of the EPR spectrum of **5** in the reaction mixtures in Scheme 6 indicates that the formation of this paramagnetic derivative (Scheme 7) is probably caused by the additional bimolecular dealkylation of unstable **7** with oxygen or sulfur.

In a similar manner, the monophenyl-substituted tin compound **4** (Scheme 7) could be generated by dephenylation of the intermediate diradical complex **3** with sulfur or some

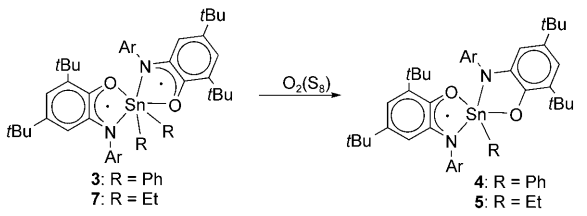

Scheme 7. The dearylation and dealkylation of diradical complexes **3** and **7**.

phenyltin sulfide derivative to give bis(triphenyltin) sulfide as a final product. The dealkylation of alkyltin and dearylation of aryltin compounds with sulfur and tin mercaptides is known.[8] The phenyl substituent in **3** is not lost spontaneously upon heating its toluene solutions at 80 °C for several hours.

Molecular structure of 3, 4, and 6: Molecular structures of **3**, **4**, and **6** are shown in Figures 4–7. Selected bond lengths and angles are given in Table 1 and the crystal data collection and structure refinement data in Table 2. Crystals of **3**, **4** and **6** suitable for X-ray analysis were obtained from hexane.

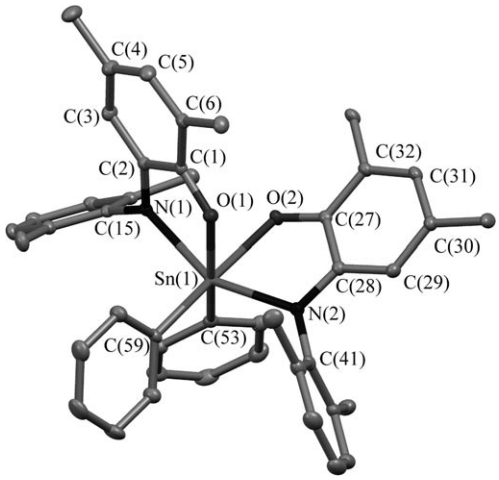

Figure 4. Molecular structure of **3** with 30% thermal probability ellipsoids. H atoms and methyl groups of *t*Bu and *i*Pr substituents are omitted for clarity.

The central tin atom in **3** (Figure 4) has a distorted octahedral environment composed of two O,N-coordinated *o*-iminobenzosemiquinonato ligands and two phenyl groups. The angle between the *o*-iminosemiquinoid ligands is 57.02°. The centroid-to-centroid distance between these radical anions, 5.085 Å, is in good agreement with the radical separation calculated from EPR data (5.10 Å).

The Sn(1)–O(1), Sn(1)–O(2), Sn(1)–N(1), and Sn(1)–N(2) distances (2.1689(14), 2.1642(14), 2.2643(16), and 2.2676(17) Å, respectively) are close to those obtained for a known Sn^{IV} *o*-iminosemiquinonate complex.[6] The Sn(1)–C-

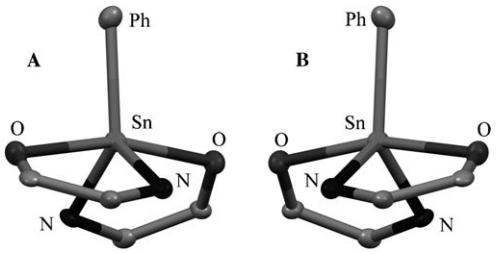

Figure 5. Fragments of structures of two independent units in the crystal of **4** with 40% thermal probability ellipsoids.

(53,59) bond lengths (2.1543(6) and 2.167(2) Å, respectively) of Sn–Ph fragments are in the typical range for related compounds containing a six-coordinated tin atom and two chelated N,O-ligands.[11]

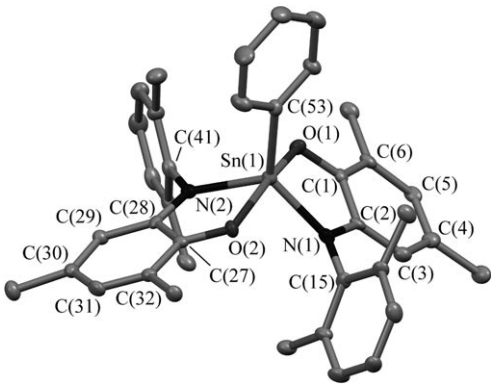

Figure 6. Molecular structure of **4** with 40% thermal probability ellipsoids. H atoms and methyl groups of *t*Bu and *i*Pr substituents are omitted for clarity.

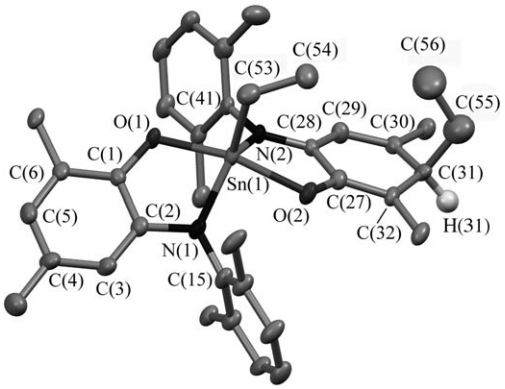

Figure 7. Molecular structure of **6** with 30% thermal probability ellipsoids. H atoms and methyl groups of *t*Bu and *i*Pr substituents are omitted for clarity.

The C–O and C–N bond lengths of the *o*-iminoquinone ligands in **3** (Table 1) are indicative of O,N-coordinated *o*-iminobenzosemiquinonato radical anions (C–O 1.29–1.33 Å, C–N 1.33–1.45 Å).[12] These bonds in **3** are significantly shorter than expected for a coordinated *o*-amidophenolate (C–O 1.35–1.36 Å, C–N 1.38–1.39 Å) or its N-protonated *o*-aminophenolate form (C–O 1.35–1.36 Å, C–N 1.42–1.47 Å).[12,13] In addition, nitrogen atoms are three-coordinated and sp^2-hybridized, and the sums of the angles about the nitrogen atoms are 359.9(4)° and 359.8(4)°. In both ligands the six ring C atoms in the *o*-iminobenzosemiquinonato part are not equidistant and show quinoid-type alternation, whereas the six C–C interatomic distances in the *N*-phenyl part are the same (1.39 ± 0.01 Å) within experimental error.

Table 1. Selected bond lengths [Å] and angles [°] of complexes **3**, **4**, and **6**.

	3	**4**	**6**
Sn(1)–O(1)	2.1689(14)	2.025(2)	2.034(2)
Sn(1)–O(2)	2.1642(14)	2.126(2)	2.083(2)
Sn(1)–N(1)	2.2643(16)	2.021(3)	2.029(3)
Sn(1)–N(2)	2.2676(17)	2.135(3)	2.164(3)
Sn(1)–C(53)	2.1543(10)	2.130(4)	2.139(4)
Sn(1)–C(59)	2.167(2)	–	–
N(1)–C(2)	1.340(2)	1.400(5)	1.417(5)
N(1)–C(15)	1.442(2)	1.437(5)	1.428(5)
N(2)–C(28)	1.340(2)	1.342(5)	1.341(4)
N(2)–C(41)	1.449(2)	1.452(5)	1.438(4)
O(1)–C(1)	1.292(2)	1.361(4)	1.353(4)
O(2)–C(27)	1.303(2)	1.295(4)	1.335(4)
C(1)–C(2)	1.463(3)	1.424(5)	1.429(5)
C(1)–C(6)	1.432(3)	1.398(5)	1.399(5)
C(2)–C(3)	1.421(3)	1.382(5)	1.359(5)
C(3)–C(4)	1.367(3)	1.393(5)	1.393(5)
C(4)–C(5)	1.430(3)	1.383(6)	1.405(6)
C(5)–C(6)	1.376(3)	1.408(5)	1.416(6)
C(27)–C(28)	1.458(3)	1.463(5)	1.464(5)
C(27)–C(32)	1.428(3)	1.439(5)	1.378(5)
C(28)–C(29)	1.429(3)	1.418(5)	1.416(5)
C(29)–C(30)	1.368(3)	1.362(5)	1.351(5)
C(30)–C(31)	1.425(3)	1.425(6)	1.478(5)
C(31)–C(32)	1.376(3)	1.369(5)	1.454(5)
O(1)-Sn(1)-N(1)	73.66(5)	81.71(11)	81.48(11)
O(1)-Sn(1)-N(2)	84.76(5)	92.97(11)	90.80(10)
O(2)-Sn(1)-N(1)	84.94(5)	91.33(11)	90.27(11)
O(2)-Sn(1)-N(2)	73.40(5)	76.40(11)	76.84(10)
O(2)-Sn(1)-O(1)	77.86(5)	163.12(9)	157.67(10)
C(53)-Sn(1)-N(1)	94.07(6)	129.39(14)	122.03(15)
C(53)-Sn(1)-N(2)	103.19(6)	113.49(13)	113.25(14)
C(53)-Sn(1)-O(1)	163.78(6)	101.45(12)	101.52(13)
C(53)-Sn(1)-O(2)	90.74(6)	94.86(12)	100.45(13)
C(59)-Sn(1)-N(1)	100.11(6)	–	–
C(59)-Sn(1)-N(2)	96.90(6)	–	–
C(59)-Sn(1)-O(1)	89.51(6)	–	–
C(59)-Sn(1)-O(2)	164.58(6)	–	–
N(1)-Sn(1)-N(2)	152.24(6)	116.79(12)	124.64(12)
C(1)-O(1)-Sn(1)	117.55(11)	112.8(2)	112.6(2)
C(27)-O(2)-Sn(1)	116.27(11)	115.4(2)	116.2(2)
C(2)-N(1)-C(15)	119.41(15)	119.0(3)	119.3(3)
C(2)-N(1)-Sn(1)	114.18(12)	112.5(2)	112.2(2)
C(15)-N(1)-Sn(1)	126.40(12)	127.4(2)	128.4(2)
C(28)-N(2)-C(41)	118.74(15)	120.9(3)	121.0(3)
C(28)-N(2)-Sn(1)	113.03(12)	115.3(2)	113.6(2)
C(41)-N(2)-Sn(1)	128.00(11)	123.7(2)	125.3(2)
C(53)-Sn(1)-C(59)	103.32(7)	–	–
C(30)-C(31)-C(55)	–	–	108.4(3)
C(30)-C(31)-C(32)	–	–	119.4(3)
C(30)-C(31)-H(31)	–	–	108.6(3)
C(32)-C(31)-C(55)	–	–	102.6(3)

Table 2. Summary of crystal and refinement data for complexes **3, 4** and **6**.

	3	**4**	**6**
formula	$C_{64}H_{84}N_2O_2Sn$	$C_{58}H_{79}N_2O_2Sn$	$C_{59}H_{91}N_2O_2Sn$
M_r	1032.02	954.92	979.03
T [K]	150(2)	100(2)	130(2)
λ [Å]	0.71073	0.71073	0.71073
crystal system	triclinic	monoclinic	monoclinic
space group	$P\bar{1}$	$P2_1$	$P2_1/n$
a [Å]	12.782(5)	13.0375(4)	11.7267(7)
b [Å]	13.947(5)	32.1455(10)	23.0975(14)
c [Å]	16.552(5)	13.3604(4)	20.3931(13)
α [°]	86.759(5)	90	90
β [°]	85.687(5)	102.5110(10)	93.9410(10)
γ [°]	79.261(5)	90	90
V [Å^3]	2888.1(18)	5466.3(3)	5510.6(6)
Z	2	4	4
ρ_{calcd} [g cm^{-3}]	1.187	1.160	1.180
μ [mm^{-1}]	0.485	0.507	0.504
crystal size [mm]	0.42×0.19×0.16	0.25×0.16×0.05	0.32×0.15×0.14
θ range [°]	2.97–28.76	2.08–26.00	2.07–23.75
reflns collected	29523	46999	38045
independent reflns	13017 [R(int) = 0.0282]	21245 [R(int) = 0.0636]	8346 [R(int) = 0.0763]
completeness (to θ)	99.8% (28.76)	99.8% (26.00)	99.4% (23.75)
absorption correction	none	semi-empirical from equivalents	semi-empirical from equivalents
max/min transmission	–	0.9751/0.8837	0.9327/0.8552
refinement method	full-matrix least-squares on F^2	full-matrix-block least-squares on F^2	full-matrix least-squares on F^2
data/restraints/parameters	13017/0/642	21245/1/1135	8346/25/605
final R indices [$I>2\sigma(I)$][a,b]	$R1$ = 0.0310 $wR2$ = 0.0722	$R1$ = 0.0497 $wR2$ = 0.0845	$R1$ = 0.0606 $wR2$ = 0.1442
R indices (all data)	$R1$ = 0.0423 $wR2$ = 0.0774	$R1$ = 0.0796 $wR2$ = 0.0913	$R1$ = 0.0972 $wR2$ = 0.1589
goodness-of-fit on F^2	1.025	0.966	1.031

[a] $R = \Sigma ||F_o| - |F_c|| / \Sigma |F_o|$. [b] $\omega R = R(\omega F^2) = \{\Sigma[\omega(F_o^2 - F_c^2)^2] / \Sigma[\omega(F_o^2)^2]\}^{1/2}$; $\omega = 1/[\sigma^2(F_o^2) + (aP)^2 + bP]$, $P = [2F_c^2 + \max(F_o,0)]/3$.

It is noteworthy that the phenyl groups are in the *cis* position to each other, and the bond angle C(53)-Sn(1)-C(59) is 103.32(7)°. At the same time, *o*-iminosemiquinonato ligands are situated so that the nitrogen atoms are in the *trans* position and the N(1)-Sn(1)-N(2) angle is 165.24(6)° (Figure 4). It is remarkable that the *cis* position of the nitrogen atoms could lead to a significant increase in steric repulsion between the 2,6-diisopropylphenyl ligands.

There are two crystallographically unique molecules in the asymmetric unit of **4.** The presence of two asymmetric chelated rings in the five-coordinated tin(IV) complex assumes chirality of the metal center and both isomers (**A** and **B**) are present in the unit cell of **4** (Figure 5). The angles and bond lengths of these two units are similar and therefore only the B molecule is discussed here.

The five-coordinated Sn atom in complex **4** has a distorted trigonal bipyramidal environment (Figures 5 and 6). The nitrogen atoms and phenyl group form the pyramid base and the oxygen atoms occupy apical sites. It is noteworthy that the phenyl group is shifted from N(1) to N(2) in a hypothetical N(1)-C(53)-Sn(1)-N(2) plane (the sum of bond angles N(1)-Sn(1)-C(53), N(2)-Sn(1)-C(53), and N(1)-Sn(1)-N(2) is 359.7(4)°): the angles N(1)-Sn(1)-C(53) and N(2)-Sn(1)-C(53) are 129.39(14)° and 113.49(13)°, respectively. The heteroatom-to-tin-to-heteroatom angles reveal the difference usual for five-coordinated transition-metal complexes of the ML_2X type[12] (L = *o*-iminobenzoquinonato-based ligand): N(1)-Sn(1)-N(2) = 116.79(12)° < O(1)-Sn(1)-O(2) = 163.12(9)°, whereas in the germanium complex [Ge(ap)Cl(isq)] an increase in the O-M-O angle compared with N-M-N was observed.[13] The angle between *o*-iminoquinoid ligands is 59.13°.

One of the *o*-iminoquinoid ligands in **4** is the *o*-amidophenolate dianion. The O(1)–C(1) (1.361(4) Å) and N(1)-N(2) distances (1.400(5) Å) are close to those in *o*-amidophenolatotin(IV) complexes.[6,14] The C(1)–C(6) carbon ring has aromatic character with an average C–C distance of 1.40±0.02 Å.

The second ligand shows the features of an *o*-iminosemiquinonato ligand. The N(2)–C(28) (1.342(5) Å) and O(2)–C(27) (1.295(4) Å) bonds are significantly longer than N(1)–C(2) and O(1)–C(1) and they are typical of *o*-iminosemiquinonato metal complexes.[12] Moreover, the six-membered C(27)–C(32)carbon ring is quite distorted. The quinoid pattern is observed: two shorter bonds are separated by longer bonds (Table 1).

The Sn(1)–O(1) and Sn(1)–N(1) covalent bonds (2.025(2) and 2.021(3) Å, respectively) are considerably shorter than Sn(1)–O(2) and Sn(1)–N(2) (2.126(2) and 2.135(2) Å, respectively), which is indicative of the different nature of *o*-iminoquinoid ligands. The longer Sn–N and Sn–O bonds are characteristic of the radical anion form of the ligand. The Sn(1)–C(53) distance (2.130(4) Å) is slightly shorter than analogous bonds in **3** due to the decrease in the metal coordination number from six to five.

The tin atom in **6** has a trigonal bipyramidal environment (Figure 7). The nitrogen atoms and phenyl group form the pyramid base and oxygen atoms occupy apical sites. Similarly to **4**, the alkyl substituent on the tin atom is shifted from N(1) to N(2) in a hypothetical N(1)-C(53)-Sn(1)-N(2) plane (the sum of bond angles N(1)-Sn(1)-C(53), N(2)-Sn(1)-C(53), and N(1)-Sn(1)-N(2) is 359.9(4)°): the angles N(1)-Sn(1)-C(53) and N(2)-Sn(1)-C(53) are 122.03(15)° and 113.25(14)°, respectively. The heteroatom-to-tin-to-heteroa-

tom angles show the same relationship: N(1)-Sn(1)-N(2) (124.64(12)°) is less than O(1)-Sn(1)-O(2) (157.67(10)°).

The complex **6** demonstrates the presence of two different chiral tin atoms in the unit cell, as in the case of **4**, but the attachment of the ethyl group to the carbon atom causes another optically isomeric atom (C(31)) to appear in the molecule. However, only one isomer per chiral carbon atom is present in the unit cell of **6**.

One of the chelated ligands in **6** is an *o*-amidophenolate dianion. Its geometric characteristics are close to those observed for such ligands bonded to nontransition[4,6,13,14] or transition[12] metal atoms. The second ligand in **6** is the first example of iminocyclohexa-1,4-dienolate derivatives to be reported. The C(27)–C(32) carbon ring contains a quaternary carbon atom, C(31). The angles around this carbon atom indicate its tetrahedral geometry. The C(27)–C(32) and C(29)–C(30) bonds (1.378(5) and 1.351(5) Å) are shorter than the usual bonds in aromatic rings and apparently have double character, whereas the other bonds C(27)–C(28), C(28)–C(29), C(30)–C(31), and C(31)–C(32) (1.464(5), 1.416(5), 1.478(5), and 1.454(5) Å) are considerably longer. This bond length distribution is close to those observed for the rare structurally characterized osmium carbonyl complex containing a π-bonded iminocyclohexa-1,4-diene ligand,[15a] and the cyclohexadienyliminatonickel complex.[15b] The C(28)–N(2) bond length (1.341(4) Å) is significantly shorter than C(2)–N(2) and close to C···N in the *o*-iminosemiquinolate ligands of **3** and **4**.

The Sn(1)–O(1) and Sn(1)–N(1) distances (2.034(2) and 2.029(3) Å) in **6** are typical of *o*-amidophenolate tin(IV) derivatives.[6,14]

The Sn(1)–N(2) bond (2.164(3) Å) is longer than the sum of the covalent radii of nitrogen and tin (2.12 Å[16]) but shorter than the sum of the van der Waals radii of these elements (3.8 Å,[16]) which is indicative of the donor–acceptor nature of the tin–imine nitrogen bond. The Sn(1)–C(53) bond length (2.139(4) Å) of Sn–Et fragments is close to the distance observed for a five-coordinated ethyltin derivative containing a tridentate ONO ligand.[17]

There are intramolecular H···π contacts (< 3.05 Å[18]) in **3**, **4**, and **6**. They are caused by the sterically bulky ligands in the coordination sphere of tin, which contains a π system of double bonds. In **3**, H(Me)···π interactions between one hydrogen atom of the CH_3(*i*Pr) groups in the *o*-iminosemiquinonato ligands and the centers of the phenyl ligands (2.76, 2.90 Å) are observed. In contrast to **3**, **4** does not contain intramolecular H···π contacts with the phenyl ligands, but there are H···π interactions between the centers of the 2,6-diisopropylphenyl ligands and the hydrogen atoms of the *tert*-butyl groups of the isq and ap substituents (≈2.90 Å).

The most interesting situation is observed for complex **6**, in which the methyl group of the ethyl substituent on the iminocyclohexa-1,4-dienolate ligand is turned towards the six-membered C(27)–C(32) ring. The distances between the two hydrogen atoms of the CH_3 group and the centers of the double C(27)–C(32) and C(29)–C(30) bonds are 2.77 and 2.67 Å. Also, the CH_3 groups of the ethyl ligands are turned toward to each other ("Me–Me" conformation). To elucidate the role of the nonbonding interactions in the coordination sphere of tin in determining the conformation, we evaluated the nonvalence energy of rotation of the Et groups around the Sn(1)–C(53) and C(31)–C(55) bonds in **6**. For our theoretical calculations of the energy of nonvalence interactions as a function of the torsion angle (Figure 8) we used the MOLDRAW program[19–21] and the geometry of **6** in the crystal state. The theoretical energy minima in **6** are close to the experimentally observed torsion angles (O(1)-Sn(1)-C(53)-C(54) 209.0(3)°, C(32)-C(31)-C(55)-C(56) 296.7(6)°). The rotation of the Et group around the C(31)–C(55) bond (Figure 8) leads to unequal energy minima (127°, 74.7 kJ mol^{-1}; 287°, 1.3 kJ mol^{-1}). Despite the clear difference between the torsion angles for minimum energy (287°) and the value observed in the complex (296.7(6)°), the energy values differ only slightly (1.3 and 1.5 kJ mol^{-1}, respectively). Two approximately equal energy minima (Figure 8) are observed for the rotation of the second Et group around the Sn(1)–C(53) bond (at 29°, −2.3 kJ mol^{-1}; at 209°, 2.2 kJ mol^{-1}). Therefore two different orientations of the Et group at the Sn atom probably exist in the molecule of complex **6**.

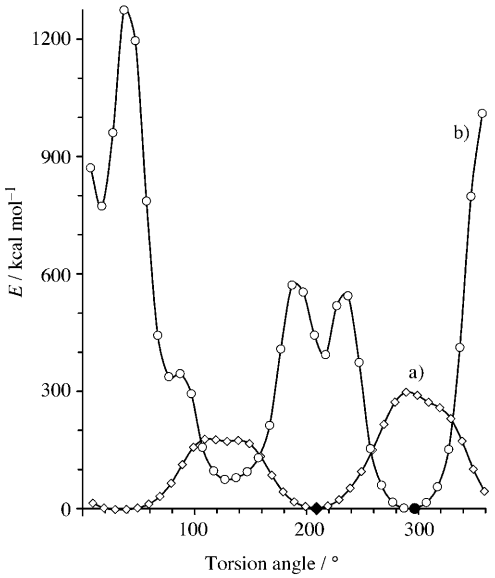

Figure 8. The energy barrier for rotation of the Et group a) about the Sn(1)–C(53) bond and b) the C(31)–C(55) bond in complexes **6**. The filled points are experimentally observed torsion angles.

Conclusion

Tin complexes have been shown to simulate some of the properties of transition-metal derivatives, owing to the coordination of the tin metal with the redox-active *o*-amidophenolate ligand. The reaction of diorganotin(IV) *o*-amidophenolate complexes with oxygen and sulfur leads to the oxida-

tion of the *o*-amidophenolate to the *o*-iminosemiquinolate ligand. Probable schemes for these reactions are proposed. The interaction with molecular oxygen includes intermediate metal μ-peroxo derivatives which undergo rearrangement; formation of new *o*-iminoquinonate tin(IV) derivatives were observed as a result.

Experimental Section

General aspects: Infrared spectra of complexes in the 4000–400 cm^{-1} range were recorded by using a Specord M-80 spectrophotometer in Nujol. The NMR spectrum of **6** was recorded in C_6D_6 solution by using a Bruker Avance III 400 MHz instrument with TMS as internal standard. EPR spectra were recorded by using a Bruker EMX spectrometer (working frequency ≈ 9.75 GHz). The g_i values were determined using 2,2-diphenyl-1-picrylhydrazyl (DPPH) as the reference ($g_i = 2.0037$). EPR spectra of **3**, **4**, and **5** were simulated with the WinEPR SimFonia Software (Bruker). The elemental analysis was performed on an Elemental Analyzer Euro EA 3000 instrument.

All reagents were spectroscopic grade. Solvents were purified by standard methods.[22] All manipulations on complexes were carried out under conditions excluding air, oxygen, and moisture. Complexes **1** and **2**,[6] dichlorodiethyltin(IV),[8] ImQ,[9] and *o*-iminosemiquinolate lithium derivative[13] were synthesized by known procedures.

Reaction of 1 with oxygen: The degassed solution of complex **1** (0.9 g, 1.38 mmol) in toluene (30 mL) in a 100 mL ampoule was filled with dry oxygen (30.9 mL, 1.38 mmol) and the reaction mixture was stirred for 1 h. The reaction was accompanied by a color change from yellow to deep green and precipitation of a white deposit. The mixture was degassed and the subsequent procedures were performed under anaerobic conditions. The precipitate (0.16 g, 0.56 mmol, 81 %) was collected on a glass filter and characterized as a diphenyltin(IV) oxide polymer.[8] The filtrate was evaporated and the residue was recrystallized from hot hexane (20 mL). Deep green crystals of complex **3** (0.53 g, 0.51 mmol, 74 %) were obtained.

Bis(4,6-di-tert-*butyl*-N-*(2,6-diisopropylphenyl)*-o-*iminobenzosemiquinonato)diphenyltin(IV) (**3**)*: Deep green crystals, soluble in most organic solvents. IR (Nujol): $\tilde{\nu} = 3057$ (m), 1586 (m), 1430 (vs), 1354 (s), 1329 (s), 1252 (s), 1197 (w), 1165 (m), 1113 (w), 1103 (w), 1070 (w), 1026 (w), 992 (w), 910 (w), 883 (s), 798 (s), 767 (w), 698 (m), 497 cm^{-1} (w); elemental analysis calcd (%) for $C_{64}H_{84}N_2O_2Sn$ (1032.56): C 74.48, H 8.20; N 2.71, Sn 11.50; found: C 74.25, H 8.10, N 2.79, Sn 11.45.

Reaction of 1 with sulfur: The degassed solution of complex **1** (0.9 g, 1.38 mmol) in toluene (30 mL) in a 100 mL ampoule was added to a sulfur (0.044 g, 1.38 mmol) suspension in the same solvent and the reaction mixture was stirred at 60 °C for 8 h. The reaction was accompanied by a color change from yellow to green. The resulting solution was evaporated and dissolved in hot hexane (50 mL). The solution was concentrated and white needle-shaped crystals were precipitated. This deposit was decanted from the mother liquor, recrystallized from hot acetonitrile, and characterized by elemental analysis, melting point, IR and ^{1}H NMR spectroscopy to be the already known bis(triphenyltin) sulfide[8] (0.17 g, 0.23 mmol, 66 %). The cooling of the residual solution to −18 °C led to precipitation of green crystals of complex **4** (0.39 g, 0.41 mmol, 59 %).

(4,6-Di-tert-*butyl*-N-*(2,6-diisopropylphenyl)*-o-*amidophenolato)-(4,6-di*-tert-*butyl*-N-*(2,6-diisopropylphenyl)*-o-*iminobenzosemiquinonato)phenyltin(IV) (**4**)*: Green crystals, soluble in most organic solvents. IR: $\tilde{\nu}$1582 (m), 1567 (m), 1431 (vs), 1416 (s), 1361 (w), 1332 (m), 1283 (w), 1256 (w), 1238 (s), 1219 (w), 1200 (w), 1168 (w), 1103 (w), 1057 (w), 991 (s), 931 (w), 912 (w), 864 (w), 850 (w), 821 (w), 804 (m), 765 (w), 696 (w), 653 (w), 609 (w), 547 (w), 500 cm^{-1} (w); elemental analysis calcd (%) for $C_{58}H_{79}N_2O_2Sn$ (954.97): C 72.95, H 8.34, N 2.93, Sn 12.43; found: C 73.04, H 8.49, N 2.75, Sn 12.27.

Reaction of 2 with oxygen: A 100 mL ampoule containing a degassed solution of **2** (0.9 g, 1.37 mmol) in toluene (30 mL) was filled with dry oxygen (30.7 mL, 1.37 mmol) and the reaction mixture was stirred for 1 h. The color changed from yellow to green-brown and a white precipitate was deposited during the reaction. The reaction mixture was degassed and the subsequent procedures were performed under anaerobic conditions. The precipitate (0.11 g, 0.57 mmol, 83 %) was collected on a glass filter and characterized as diethyltin(IV) oxide polymer.[8] The filtrate was evaporated and the residue was recrystallized from hexane (20 mL). Brown crystals of **6** (0.36 g, 0.35 mmol, 51 %) were obtained.

(4,6-Di-tert-*butyl*-N-*(2,6-diisopropylphenyl)*-o-*amidophenolato)(2,4-di*-tert-*butyl-6-(2,6-diisopropylphenylimino)-3-ethylcyclohexa-1,4-dienolato)ethyltin(IV) hexane solvate (**6**)*: Brown crystals, soluble in most organic solvents. ^{1}H NMR (20 °C, C_6D_6): $\delta = 0.34$ (t, $J_{H,H} = 6.7$ Hz, 3H; CH_3 of Et−Sn), 0.67 (s, 9H; CH_3 of *t*Bu), 1.08 (s, 9H; CH_3 of *t*Bu), 1.09 (d, $J_{H,H} = 6.7$ Hz, 6H; CH_3 of *i*Pr), 1.22 (d, $J_{H,H} = 6.7$ Hz, 6H; CH_3 of *i*Pr), 1.28 (s, 9H; CH_3 of *t*Bu), 1.39 (s, 9H; CH_3 of *t*Bu), 1.44 (t, $J_{H,H} = 6.7$ Hz, 3H; CH_3 of Et), 1.45 (d, $J_{H,H} = 6.7$ Hz, 6H; CH_3 of *i*Pr), 1.48 (d, $J_{H,H} = 6.7$ Hz, 6H; CH_3 of *i*Pr), 1.67 (m, 2H; CH_2 of Et−Sn), 1.72 (m, 2H; CH_2 of Et), 2.99 (m, 2H; CH of *i*Pr), 3.63 (m, 2H; CH of *i*Pr), 3.63 (m, 1H; CH of C(Et)H), 6.15 (s, 1H; CH−aromatic), 6.31 (d, $J_{H,H} = 2.2$ Hz, 1H; CH-aromatic), 6.85 (d, $J_{H,H} = 2.2$ Hz, 1H; CH−-aromatic), 7.04–7.18 (m, 3H; CH−aromatic), 7.25–7.36 ppm (m, 3H; CH−aromatic); ^{13}C NMR (20 °C, C_6D_6): $\delta = 5.58$, 9.76, 14.67 ($J^1(^{13}C-^{119}Sn) = 857$ Hz), 24.19, 24.46, 24.75, 25.03, 25.28, 25.37, 25.38, 25.82, 26.12, 28.21, 28.47, 28.68, 28.77, 28.89, 29.85, 30.25, 32.27, 34.61, 35.14, 36.22, 37.09, 43.83, 107.53, 110.36, 117.55, 123.81, 124.15, 124.48, 125.33, 126.00, 128.06, 132.33, 137.83, 138.04, 138.99, 141.20, 141.80, 142.10, 143.39, 147.80, 147.80, 148.34, 148.36, 167.24, 175.57 ppm; ^{119}Sn NMR (20 °C, C_6D_6): $\delta = -206.32$ ppm (assignment of NMR signals was defined more exactly using 2D ge-COSY (ge = gradient-enhanced) and ge-HSQC NMR); IR: $\tilde{\nu} = 1615$ (w), 1565 (s), 1511 (s), 1429 (s), 1416 (s), 1360 (m), 1331 (m), 1282 (m), 1257 (w), 1238 (s), 1220 (s), 1102 (w), 1056 (w), 990 (m), 927 (w), 905 (w), 886 (w), 872 (w), 850 (w), 822 (w), 800 (m), 766 (w), 677 (w), 626 (w), 609 (w), 585 (w), 546 (w), 500 (w), 424 cm^{-1} (w); elemental analysis calcd (%) for $C_{62}H_{98}O_2N_2Sn$ (1022.16): C 72.85, H 9.66, N 2.74, Sn 11.61; found: C 72.95, H 9.50, N 2.85, Sn 11.75 %.

Reaction of 2 with sulfur: The degassed solution of complex **2** (0.9 g, 1.37 mmol) in toluene (30 mL) in a 100 mL ampoule was added to a sulfur (0.044 g, 1.37 mmol) suspension in the same solvent and the reaction mixture was stirred at 60 °C for 8 h. The reaction was accompanied by color change from yellow to light green. The resulting solution was evaporated and recrystallized from hexane (20 mL). The crystals obtained were characterized as complex **6** (0.34 g, 0.33 mmol, 49 %).

Complexes **5** and **7** were investigated in solution by EPR spectroscopy and were not isolated as solids.

X-ray crystallography of 3, 4, and 6: Crystals of **3, 4**, and **6** suitable for X-ray structure determination were obtained from hexane solution. Intensity data for **3**, **4**, and **6** were collected on a Smart Apex diffractometer with graphite monochromated $Mo_{K\alpha}$ radiation ($\lambda = 0.71073$ Å) in the ϕ--ω scan mode ($\omega = 0.3°$, 10 s on each frame). The intensity data were integrated by the SAINT program.[23] SADABS[24] was used to perform area-detector scaling and absorption corrections. The structures were solved by direct methods and were refined on F^2 using all reflections with the SHELXTL package.[25] All non-hydrogen atoms were refined anisotropically. Hydrogen atoms were placed in calculated positions and refined in the "riding model" ($U_{iso}(H) = 1.5U_{eq}(C)$ in CH_3 groups; $U_{iso}(H) = 1.2U_{eq}(C)$ in other ligands). A molecule of hexane in **6** was positioned in the inversion center. Selected bond distances and angles for **3**, **4**, and **6** are given in Table 1. CCDC-689153 (**3**), 689154 (**4**), and 689155 (**6**) contain the supplementary crystallographic data for this paper. These data can be obtained free of charge from www.ccdc.cam.ac.uk/conts/retrieving.html or from The Cambridge Crystallographic Data Centre via www.ccdc.cam.ac.uk/data_request/cif.

Acknowledgements

We are grateful to the Russian Foundation for Basic Research (grants 07-03-00711-a, 07-03-00819-a, and 06-03-32728-a) and the Russian President Grant (grant NSh-4182.2008.3) for financial support of this work.

[1] a) I. L. Fedushkin, V. M. Makarov, E. C. E. Rosenthal, G. K. Fukin, *Eur. J. Inorg. Chem.* **2006**, 827–832; b) I. L. Fedushkin, A. A. Skatova, G. K. Fukin, M. Hummert, H. Schumann, *Eur. J. Inorg. Chem.* **2005**, 2332–2338; c) I. L. Fedushkin, A. G. Morozov, O. V. Rassadin, G. K. Fukin. *Chem. Eur. J.* **2005**, *11*, 5749–5757; d) I. L. Fedushkin, N. M. Khvoinova, A. A. Skatova, G. K. Fukin, *Angew. Chem.* **2003**, *115*, 5381–5384; *Angew. Chem. Int. Ed.* **2003**, *42*, 5223–5226; e) I. L. Fedushkin, A. A. Skatova, M. Hummert, H. Schumann, *Eur. J. Inorg. Chem.* **2005**, 1601–1608.

[2] a) B. Tumanskii, P. Pine, Y. Apeloig, N. J. Hill, R. West, *J. Am. Chem. Soc.* **2006**, *128*, 7786–7787; b) A. Naka, N. J. Hill, R. West, *Organometallics* **2004**, *23*, 6330–6332; c) G. A. Abakumov, V. K. Cherkasov, A. V. Piskunov, I. A. Aivaz'yan, N. O. Druzhkov, *Dokl. Chem.* **2005**, *404*, 189–192; d) B. Tumanskii, P. Pine, Y. Apeloig, N. J. Hill, R. West, *J. Am. Chem. Soc.* **2005**, *127*, 8248–8249; e) A. V. Piskunov, I. A. Aivaz'yan, V. K. Cherkasov, G. A. Abakumov, *J. Organomet. Chem.* **2006**, *691*, 1531–1534; f) A. V. Lado, A. I. Poddel'sky, A. V. Piskunov, G. K. Fukin, V. N. Ikorskii, V. K. Cherkasov, G. A. Abakumov, *Inorg. Chim. Acta* **2005**, *358*, 4443–4450; g) A. V. Lado, A. V. Piskunov, V. K. Cherkasov, G. K. Fukin, G. A. Abakumov, *Russ. J. Coord. Chem.* **2006**, *32*, 173–181; h) G. A. Abakumov, V. K. Cherkasov, A. V. Lado, A. V. Piskunov, G. K. Fukin, L. G. Abakumova, *Russ. Chem. Bull.* **2006**, *115*, 1146–1154.

[3] a) E. V. Kolyakina, L. B. Vaganova, A. V. Lado, A. V. Piskunov, V. K. Cherkasov, D. F. Grishin, *Russ. Chem. Bull.* **2007**, *116*, 1363–1368; b) E. V. Kolyakina, L. B. Vaganova, A. V. Lado, A. V. Piskunov, V. K. Cherkasov, D. F. Grishin, *Polym. Sci. Ser. A* **2008**, *50*, 153–159.

[4] a) G. A. Abakumov, V. K. Cherkasov, E. V. Grunova, A. I. Poddel'sky, L. G. Abakumova, Y. A. Kurskii, G. K. Fukin, E. V. Baranov, *Dokl. Chem.* **2005**, *405*, 222–225; b) G. A. Abakumov, A. I. Poddel'sky, E. V. Grunova, V. K. Cherkasov, G. K. Fukin, Y. A. Kurskii, L. G. Abakumova, *Angew. Chem.* **2005**, *117*, 2827–2831; *Angew. Chem. Int. Ed.* **2005**, *44*, 2767–2771; c) V. K. Cherkasov, G. A. Abakumov, E. V. Grunova, A. I. Poddel'sky, G. K. Fukin, E. V. Baranov, Y. A. Kurskii, L. G. Abakumova, *Chem. Eur. J.* **2006**, *12*, 3916–3927; d) P. Chaudhuri, E. Bill, R. Wagner, U. Pieper, B. Biswas, T. Weyhermüller, *Inorg. Chem.* **2008**, *47*, 5549–5551.

[5] J. Emsley, *The Elements*, Clarendon Press, Oxford, **1991**.

[6] A. V. Piskunov, I. A. Aivaz'yan, G. A. Abakumov, V. K. Cherkasov, O. V. Kuznetsova, G. K. Fukin, E. V. Baranov, *Russ. Chem. Bull.* **2007**, *116*, 261–266.

[7] a) C. G. Pierpont, *Coord. Chem. Rev.* **2001**, *219–221*, 415–433; b) C. G. Pierpont, *Coord. Chem. Rev.* **2001**, *216–217*, 99–125; c) C. W. Lange, B. J. Conklin, C. G. Pierpont, *Inorg. Chem.* **1994**, *33*, 1276–1283.

[8] K. A. Kocheshkov, N. N. Zemlyanskii, N. I. Sheverdina, E. M. Panov, *Methods of Elementoorganic Chemistry: Germanium, Tin, Lead*, Nauka, Moscow, **1968**, 704.

[9] G. A. Abakumov, N. O. Druzhkov, Yu. A. Kurskii, A. S. Shavyrin, *Russ. Chem. Bull.* **2003**, *112*, 712–717.

[10] a) H. Mimoun in *Comprehensive Coordination Chemistry, Vol. 6: The Synthesis, Reactions, Properties and Applications of Coordination Compounds*, (Eds.: G. Wilkinson, R. D. Gillard, J. A. McCleverty), Pergamon, Oxford, **1987**, pp. 317–410; b) *Catalysis by Metal Complexes, Vol. 26: Advances in Catalytic Activation of Dioxygen by Metal Complexes*, (Ed.:L. I. Simándi), Kluwer, Boston, **2003**.

[11] a) R. Garcia-Zarracino, J. Ramos-Quinones, H. Hopfil, *J. Organomet. Chem.* **2002**, *664*, 188–200; b) D. K. Dey, M. K. Das, H. Noth, *Z. Naturforsch. B* **1999**, *54*, 145–154; c) A. Linden, T. S. B. Baul, A. Mizar, *Acta Crystallogr.Sect. E* **2005**, *61*, m27 m29.

[12] a) A. I. Poddel'sky, V. K. Cherkasov, G. A. Abakumov, *Coord. Chem. Rev.* **2008**, DOI: 10.1016/j.ccr.2008.02.004.

[13] A. V. Piskunov, I. A. Aivaz'yan, A. I. Poddel'sky, G. K. Fukin, E. V. Baranov, V. K. Cherkasov, G. A. Abakumov, *Eur. J. Inorg. Chem.* **2008**, 1435–1444.

[14] A. V. Piskunov, I. A. Aivaz′yan, G. K. Fukin, E. V. Baranov, A. S. Shavyrin, G. A. Abakumov, V. K. Cherkasov, *Inorg. Chem. Commun.* **2006**, *9*, 612–615.

[15] a) J. U. Kohler, J. Lewis, P. R. Raithby, M. A. Rennie, *Organometallics* **1997**, *16*, 3851–3854; b) G. Bai, D. W. Stephan. *Angew. Chem.* **2007**, *119, 1888–1891; Angew. Chem. Int. Ed.* **2007**, 46, 1856–1859; *Angew. Chem. Int. Ed.* **2007**, *46*, 1856–1859.

[16] S. S. Batsanov. *Russ. J. Inorg. Chem.* **1991**, *36*, 3015–3037.

[17] J. S. Casas, A. Castiñeiras, F. Condori, M. D. Couce, U. Russo, A. Sáces, R. Seoane, J. Sordo, J. M. Varela, *Polyhedron* **2003**, *22*, 53–65.

[18] M. Nishio, *CrystEngComm* **2004**, *6(27)*, 130–158.

[19] P. Ugliengo, G. Borzani, G. Chiary, *Z. Kristallogr.* **1993**, *209*, 9–16.

[20] P. Ugliengo, G. Borzani, D. Viterbo, *Z. Kristallogr.* **1988**, *185*, 712–718.

[21] P. Ugliengo, D. Viterbo, G. Borzani, *J. Appl. Crystallogr.* **1988**, *21*, 75–84.

[22] D. D. Perrin, W. L. F. Armarego, D. R. Perrin, *Purification of Laboratory Chemicals*, Pergamon, Oxford, **1980**.

[23] Bruker, SAINTPLUS Data Reduction and Correction Program v.6.02a, Bruker AXS, Madison, WI, USA, **2000**.

[24] G. M. Sheldrick, SADABS v.2.01, Bruker/Siemens Area Detector Absorption Correction Program, Bruker AXS, Madison, WI, USA, **1998**.

[25] G. M. Sheldrick, SHELXTL v.6.12, Structure Determination Software Suite, Bruker AXS, Madison, WI, USA, **2000**.

Received: June 19, 2008
Published online: September 11, 2008

